A Linear Modulation OSL Study of the Unstable Ultrafast Component in Samples from Glacial Lake Hitchcock, Massachusetts, USA

R.J. Goble[1] and T.M. Rittenour[1,2]

1. Department of Geosciences, University of Nebraska-Lincoln, 214 Bessey Hall, Lincoln, Nebraska, USA 68588-0340 (e-mail: rgoble2@unl.edu)
2. Current Address: Department of Geology, Utah State University, 4505 Old Main Hill, Logan, Utah, USA 84322

(Received 20 April 2006; in final form 14 November 2006)

Abstract
Optical ages were determined for samples from delta and sand dune deposits associated with Glacial Lake Hitchcock near Amherst, Massachusetts using the single aliquot regenerative-dose (SAR) optically stimulated luminescence (OSL) technique. However, a strong unstable ultrafast component caused initial rejection of data from a large proportion of aliquots. A linearly modulated blue OSL (LM-OSL) study was undertaken on the sample with the strongest ultrafast component, with the data modelled using the equation of Bulur et al. (2000) as 5 fast, medium and slow components, and 1 ultrafast component.

The ultrafast component dominates the LM–OSL, almost completely obscuring the fast component. As suggested by Jain et al. (2003), the thermal stability of the ultrafast component was examined, using temperatures between 180°C and 300°C (10s preheat) and extended preheats at 300°C (10-60s). Preheats of sufficient stringency to remove the ultrafast component (300ºC for ≥ 20s) also strongly depleted the fast component. The stabilities of the ultrafast and fast components were also examined as a function of low-power, short-duration continuous-wave blue-light stimulations (CW-OSL). A 3.0s, 0.35 mW.cm^{-2} (1% diode power), 125ºC preshine in combination with a 240ºC/10s preheat removed the ultrafast component, and caused significantly less fast component depletion than more stringent preheats. Data from a modified SAR procedure in which each OSL measurement is preceded by a low-power preshine have improved recycling ratios and reduced equivalent dose (D_e) errors. D_e values and resultant ages determined using the preshine-based SAR proposed here are consistent with regional age constraints on the delta and sand dune samples from Glacial Lake Hitchcock.

Keywords
Ultrafast OSL component, Linear Modulation OSL, Glacial Lake Hitchcock

Introduction
Samples of eolian and deltaic sand associated with Glacial Lake Hitchcock near Amherst, Massachusetts (Rittenour, 1999; Rittenour and Brigham-Grette, 2000; Rittenour et al. 2000) were analyzed using the single aliquot regenerative (SAR) protocol (Murray and Wintle, 2000), using sample preparations as outlined in Rittenour et al. (2003, 2005). Analysis was carried out on a Risø TL/OSL-DA-15B/C reader with blue-green (470±30 nm; maximum power 35 mW.cm^{-2}) and infrared LEDs and a 7.5-mm Hoya U340 filter (340±50 nm) (Bøtter-Jensen et al., 2000). The software version of the MiniSys code was 1.11. In screening SAR optically stimulated luminescence (OSL) data using rejection criteria, consistent problems were noted with recycling ratios and equivalent dose (D_e) errors calculated from growth curves, resulting in an unusually large scatter in equivalent dose (D_e) values and a high proportion of data discarded. The problems were traced to the presence of a strong unstable ultrafast component (Jain et al. 2003, Choi et al. 2003). A linearly modulated OSL (LM-OSL) study was undertaken on the sample showing the strongest ultrafast component (GLH-06-09-782, Table 5) to determine a method for removing this component. LM-OSL studies were carried out by ramping the stimulation light intensity from 0 to 35 mW.cm^{-2} (100% power) over 3000s (3000 channels), following a 250Gy irradiation. All LM-OSL measurements were carried out at 125°C on a single aliquot of the sample GLH-06-09-782. Because of the low sensitivity of this and other Glacial Lake Hitchcock samples, large (5 mm) aliquots of 90-125, 90-150 or 150-180 μm quartz sand were used in all OSL analyses.

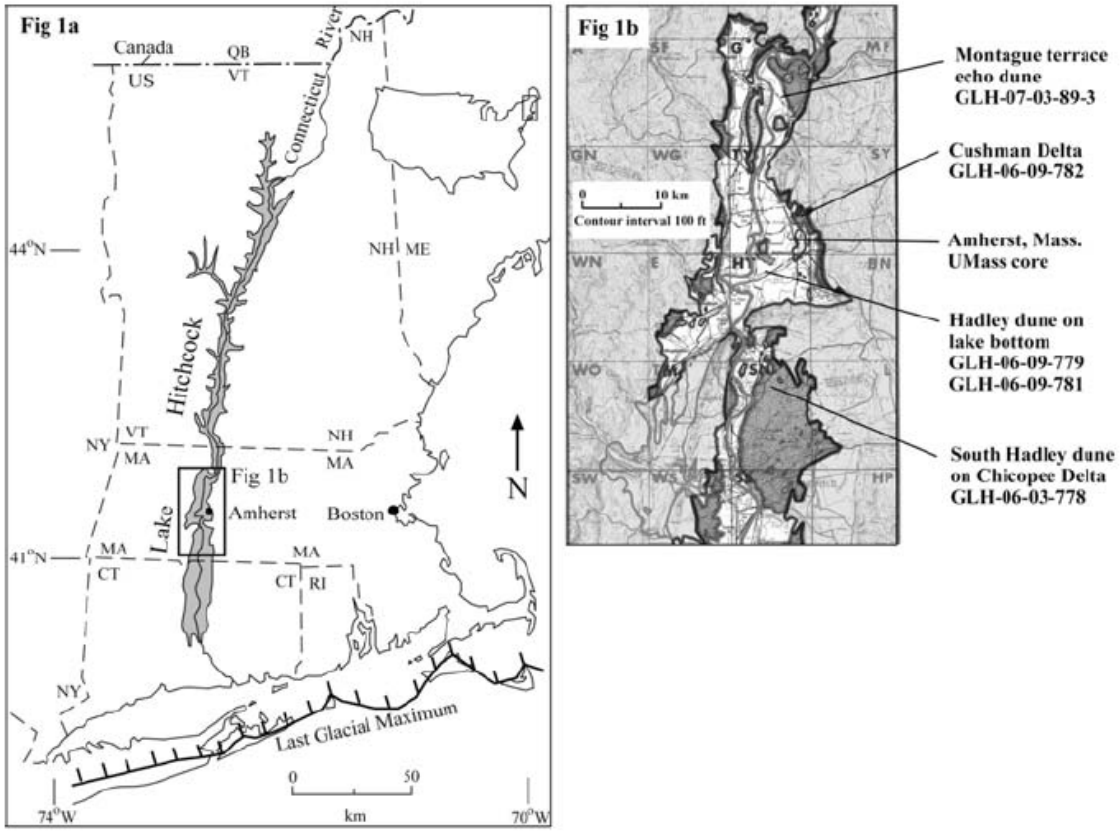

Figure 1: *Location of Glacial Lake Hitchcock within the Connecticut River valley in the northeastern United States.*

Study area

Samples for OSL dating were collected from relic delta and sand dune deposits from Glacial Lake Hitchcock, near Amherst in central Massachusetts (Figure 1). Glacial Lake Hitchcock formed in the Connecticut River valley during retreat of the Laurentide ice sheet at the close of the last glaciation. As the ice margin retreated northward, the lake formed behind a sediment dam in central Connecticut and extended 320 km to the north within the Connecticut River valley into northern Vermont. A count of annual varves from the lake basin indicates that the lake existed for over 4000 years (Antevs, 1922; Ridge et al., 1999, 2001; Rittenour, 1999). Radiocarbon age control from the New England (NE) varve chronology suggests that Glacial Lake Hitchcock formed prior to 15.0 ^{14}C kyr BP and drained by 11.8 ^{14}C kyr BP (~18.0 and ~14.0 cal kyr BP) (Ridge et al., 1999), although recent re-correlations suggest the lower portion of the NE varve chronology may be 700 years older (Ridge, 2003). During the existence of the lake, large deltas formed at the mouths of tributaries entering the lake basin. Subsequent to lake drainage, sand dunes formed on the exposed non-vegetated lake bottom, deltas and early terraces cut by the Connecticut River (Rittenour, 1999; Rittenour and Brigham-Grette, 2000). OSL samples were collected from these pre-drainage delta deposits and post-drainage eolian deposits in order to better constrain the timing of lake drainage.

Modelling of LM-OSL data

A background correction was determined by averaging the LM-OSL (3000 channels, 3000 seconds, 0 to 35 mW.cm^{-2} (100%) diode power, 125ºC) on two blank aluminium disks coated with Silkospray^{TM}. The LM-OSL background (Figure 2) shows an increase in intensity with applied power, similar to the background observed in the LM-OSL study of Choi et al. (2006); the data were fitted with a third order polynomial. A similar background, with somewhat lower intensities at higher powers was observed using a stainless steel disk during LM-OSL measurements; this finding was also checked by setting the diode power to various levels (0, 10, 20, 30…90, 100%) and measuring the background signal. These continuous wave OSL (CW-OSL) data are also shown on Figure 2, and show a similar pattern of increase. A similar CW-OSL measurement of the background using infrared diodes (125ºC) does not show the increase in intensity with power. The

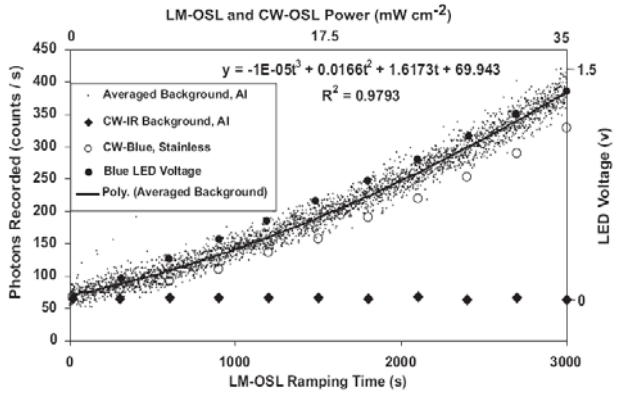

Figure 2: *LM-OSL and CW-OSL data, collected while holding the sample at 125°C, from a sample disk coated with SilkosprayTM, following 250 Gy irradiations and 240ºC/10s preheats. LM-OSL data represent the average of two measurements; CW-OSL measurements are averaged photon counts per second (100s acquisition) at the specified power (upper scale). An aluminium disk was used, unless otherwise noted in the legend. Blue LED voltages measured at the test point on the rear of the Minisys are also shown, referenced to the right-hand scale*.

voltage applied to the blue LEDs as a function of applied power is also shown in Figure 2. These data show no curvature within the error of the measurement (0.01 volts), and we conclude that the non-linearity in the background is due to increased filter breakthrough with increased power to the diodes, rather than non-linearity in the intensity of the light emitted by the LEDs. In a similar LM-OSL study, Choi et al. (2006) demonstrated that the increase in intensity of light emitted by their diodes was linear, although the background count rates from a blank disk were non-linear, and attributed the non-linearity to possible slight changes in wavelength of the LED emission with power increase, allowing more photons to pass through the filter. A background blue LM-OSL correction based on the calculated polynomial has been applied to all subsequent data sets prior to peak fitting.

LM-OSL measurements (0 – 35 mW.cm^{-2}, 3000 s, 3000 channels) were conducted on the natural GLH-06-09-782 sample and the same aliquot following a 250 Gy irradiation (Figure 3). A 240ºC/10s preheat and 125ºC measurement temperature were used. The natural signal has been multiplied by 10 for comparison purposes. The irradiated sample has a strong ultrafast component, which dwarfs the other peaks; this peak is not present in the natural sample and is thus assumed to be unstable over the age of this sample. This unstable ultrafast component is similar to that noted by Jain et al. (2003).

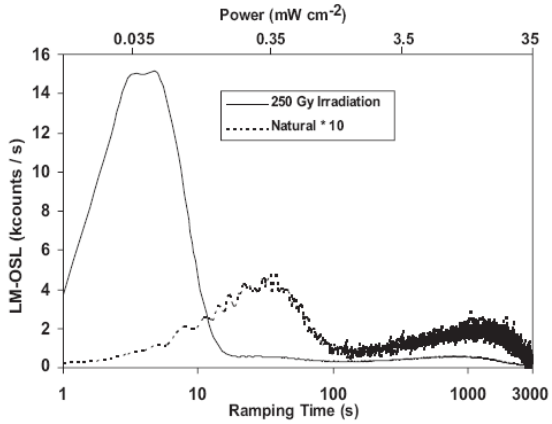

Figure 3: *Natural LM-OSL (multiplied by 10) and LM-OSL following a 250 Gy irradiation (240ºC/10s preheat, 125ºC measurement).*

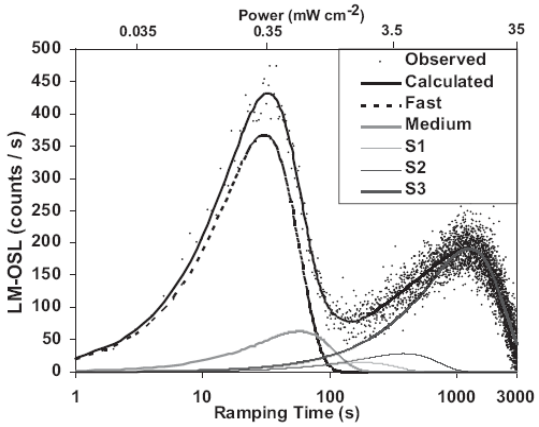

Figure 4: *Natural LM-OSL, fitted with five components using the equation of Bulur et al. (2000). Component designation follows Singarayer et al. (2003).*

The natural LM-OSL data (Figure 4) can be adequately modelled as the sum of five peaks, using the equation of Bulur et al. (2000). As shown in Table 1, relative values of σ (Choi et al., 2006) for these components are similar to those observed by Singarayer and Bailey (2003), and their notation has been followed in this study. These five peaks plus an ultrafast peak, where present, were used in fitting the data from all subsequent experiments.

Change in signal components as a function of preheat temperature

Jain et al. (2003) noted that the ultrafast component in their sample could be eliminated by heating to 260ºC; Choi et al. (2003) obtained satisfactory results using a test dose cut-heat of 220ºC. LM-OSL runs were conducted on GLH-06-09-782 between 180ºC/10s and 300ºC/10s, at 20ºC intervals, in order to determine the preheat temperature necessary for elimination of the ultrafast component (Figure 5a,

Jain et al. (2003)		Singarayer and Bailey (2003)		This Study	
Component	Relative σ	Component	Relative σ	Component	Relative σ
Ultrafast	13	Ultrafast	28	Ultrafast	27
Fast	1	Fast	1	Fast	1
Medium	0.2	Medium	0.2	Medium	0.1
Slow 1	0.06				
Slow 2	0.01	S_1	0.01	S_1	0.01
Slow 3	0.001	S_2	0.001	S_2	0.001
Slow 4	0.0001	S_3	0.0001	S_3	0.0003

Table 1: *Comparison of relative values of σ and the notation used by Jain et al. (2003), Singarayer and Bailey (2003), and this study.*

5b). The 300ºC preheat was repeated at 10 second intervals between 10 and 60s. Signal change is measured relative to the photon sum rather than the maximum photon count. Sensitivity change in the ultrafast and fast components, as monitored with a small test dose, is shown in the upper part of Figure 5b; corrections have been applied to the data in the lower part of Figure 5b (the apparent sensitivity change shown by comparing 240ºC peak intensities in Figures 3 and 5 is probably related to a changed electronic board in the Minisys). As noted by Packman et al. (in press), the ultrafast and fast components sensitize differently, particularly at temperatures above 240ºC. The ultrafast component (Figure 5b) is still present at 260ºC, but has been almost entirely removed by a 300ºC/10s preheat, although the 300ºC preheat must be maintained for at least 20 seconds (Figure 5a) to fully remove the ultrafast component. Other signal components show similar depletions with increased stringency of preheat. Increasing the preheat from 240ºC to 300ºC/20s depletes the fast component from 64±5% of the initial 180ºC intensity to 36±3%. The additional 56±6% depletion below the signal level remaining after a 240ºC preheat could be problematic in this low-response sample. Therefore, an alternate approach to removal of the ultrafast component was sought.

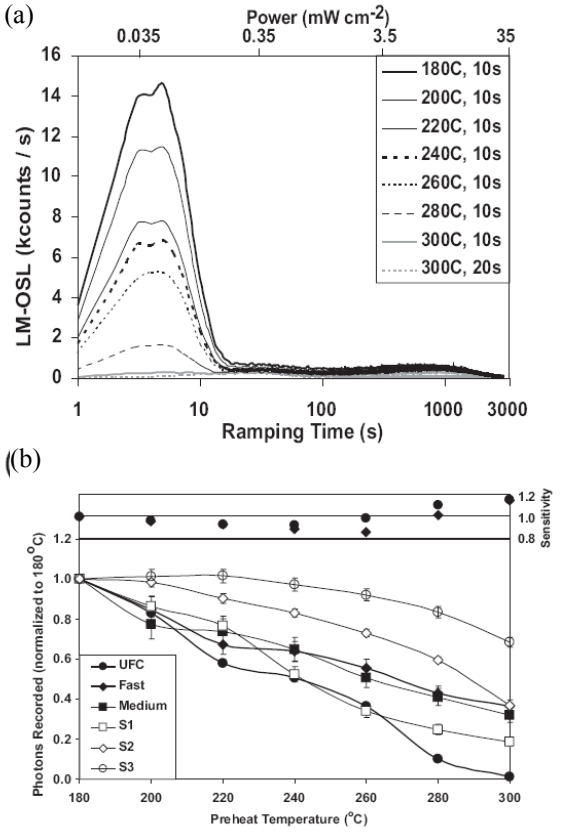

Figure 5: *a) LM-OSL following preheats at various temperatures and times (250 Gy applied dose, 125ºC measurement). b) Changes in signal strength for the six components required to model the LM-OSL signal. Changes in sensitivity for the ultrafast and fast components are shown in the upper part of the figure.*

Depletion of signal components as a function of CW-OSL power

Use of a low-power bleach to remove the ultrafast component was explored as an alternative to a more stringent preheat. The sample was given a 250 Gy dose, followed by a 240ºC/10s preheat and a 10 s CW-OSL at diode powers between 0 to 0.35 mW. cm^{-2} (1%), followed by a 3000s, 3000 channel, 0 – 35

mW.cm^{-2} (100%) diode power LM-OSL measurement at 125ºC. There was no measurable change in the LM-OSL curves below 0.5% CW-OSL power setting, or between 0.5% and 1% CW-OSL power, suggesting that the system software interprets CW-OSL values below 0.5% as 0% power and values between 0.5% and 1% as 1% power, an observation confirmed by Duller (pers. comm., 2006). With ≥ 0.35 mW.cm^{-2} (1% diode power), the ultrafast component was completely removed, and the fast component was depleted by 24±2%. This compares favourably with the 64±3% depletion associated with a preheat of sufficient stringency (300ºC/20s) to remove the ultrafast component, even allowing for the different effect of a 180ºC/10s vs 240ºC/10s preheat in these experiments. A 0.35 mW.cm^{-2} (1%) power-level setting was used for all subsequent low-power bleaching experiments. The lack of change in the LM-OSL curves through five cycles of 0% CW-OSL preshines or six cycles of 1% CW-OSL preshines also demonstrates that the long LM-OSL measurements are sufficient to remove the signal prior to the next cycle of measurements.

Depletion of signal components with CW-OSL time at 0.35 mW.cm^{-2} (1%) power

The time needed for a 1% CW-OSL preshine to remove the ultrafast component was explored by applying a 250 Gy dose, followed by a 240ºC/10s preheat and a short CW-OSL 0.35 mW.cm^{-2} (1%) power "preshine" at times from 0 to 3 seconds, followed by a 3000s, 3000 channel, 0 – 35 mW.cm^{-2} (100%) power LM-OSL at 125ºC to measure remaining peak intensities; sensitivity corrections, as determined from a small test-dose following the LM-OSL, were applied to the ultrafast and fast components. LM-OSL curves with and without a 3 second preshine are shown in Figure 6a. Changes in intensity for all components, in 0.25s time-increments, are shown in Figure 6b. Sensitivity changes in the ultrafast and fast components are shown in the upper part of Figure 6b; there is < 1% difference between the values. Decay curve data collected for the 3.0 s CW-OSL preshine are also shown. A 2.5 to 3.0 s 0.35 mW.cm^{-2} (1%) power preshine is sufficient to reduce the ultrafast component to a level similar to that observed using a 300ºC/20s preheat (~99% removed). The fast component is depleted by approximately 8±4% at 3.0s. This compares favourably with the 56±6% depletion in the fast component produced by increasing the preheat from 240ºC/10s to 300ºC/20s in order to fully remove the ultrafast component.

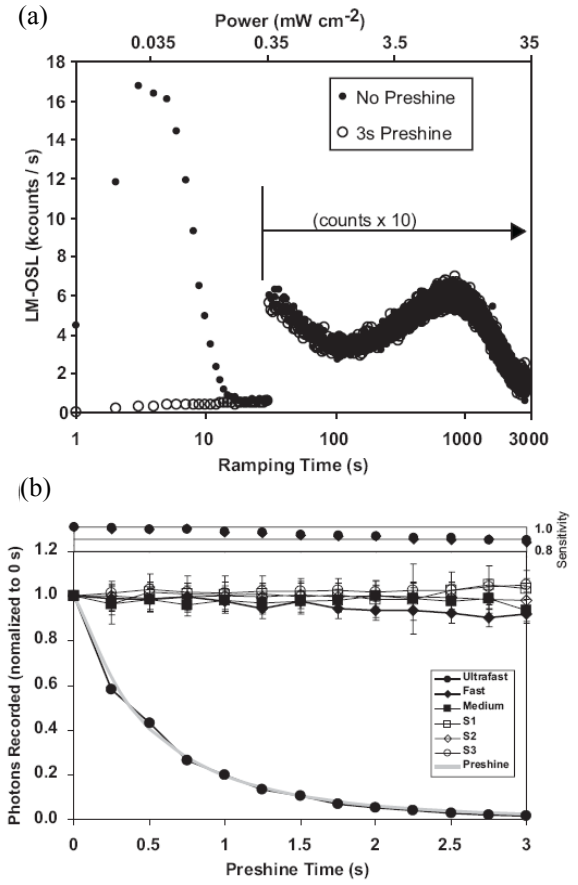

Figure 6: *a) LM-OSL with and without a 3 s, 0.35 mW cm-2 preshine (250Gy applied dose, 240ºC/10s preheat, 125ºC measurement); counts at ramping times greater than 30 s have been multiplied by 10. b) Relative change in intensity of the ultrafast and fast components as a function of CW-OSL 0.35 mW cm-2 (1%) diode power preshine times. Changes in sensitivity for the ultrafast and fast components are shown in the upper part of the figure.*

Sensitivity changes as a function of cutheat/ preheat temperature

Packman et al. (in press) have shown that sensitivity change in a sample with an ultrafast component is a function of preheat/cutheat temperature, requiring the use of the same temperature (200ºC for their samples) for both preheat and cutheat in applying the SAR procedure. This is also shown by the sensitivity data in Figure 5b. Sensitivity changes as a function of variations in cutheat and preheat temperature in sample GLH-06-09-782 were monitored by running the sequence shown in Table 2. The sensitivity change in the preshine data varies with stringency of the cutheat/preheat (Figure 7a). However, the decay-curve data measured subsequent to the preshine show

	Operation
1	200s beta (~20 Gy)
2	160°C/0s cutheat
3	2s preshine (1% power, 125ºC)
4	40s OSL (90% power, 125ºC)
5	200s beta (~20 Gy)
6	220°C/0s cutheat
7	2s preshine (1% power, 125ºC)
8	40s OSL (90% power, 125ºC)
9	200s beta (~20 Gy)
10	240°C/10s preheat
11	2s preshine (1% power, 125ºC)
12	40s OSL (90% power, 125ºC)
13	200s beta (~20 Gy)
14	260°C/10s preheat
15	2s preshine (1% power, 125ºC)
16	40s OSL (90% power, 125ºC)
	Repeat cycle (1) to (16) 3 times

Table 2: *Sequence used to determine sensitivity change with cutheat and preheat temperature. 1% power corresponds to 0.35 mW.cm^{-2}.*

	Operation
1	Apply dose (0 for natural)
2	Preheat, 260°C/10s
3	3.0s preshine CW-OSL (1% power, 125°C, 10s pause)
4	40s CW-OSL (90% power, 125°C, 10s pause)
5	Test dose irradiation
6	Cutheat, 220°C/0s
7	3.0s preshine CW-OSL (1% power, 125°C, 10s pause)
8	40s CW-OSL (90% power, 125°C, 10s pause)
9	Repeat (1) through (8) for regenerative doses
10	Calculate L_x/T_x from (4) and (8)

Table 3: *Modified SAR sequence used to remove ultrafast component. 1% power corresponds to 0.35 mW.cm^{-2}.*

little, if any, dependence on stringency of cutheat/preheat, making it unnecessary to use the same cutheat/preheat conditions if a preshine is used. The ultrafast component is most dominant in the lower temperature preheat/cutheat preshine decay curves (Figure 7b), as would be expected from the data in Figure 5 and the study by Jain et al. (2003). Therefore, unless removed by a preshine, an unstable ultrafast component will more strongly affect test-dose measurements than regenerative-dose

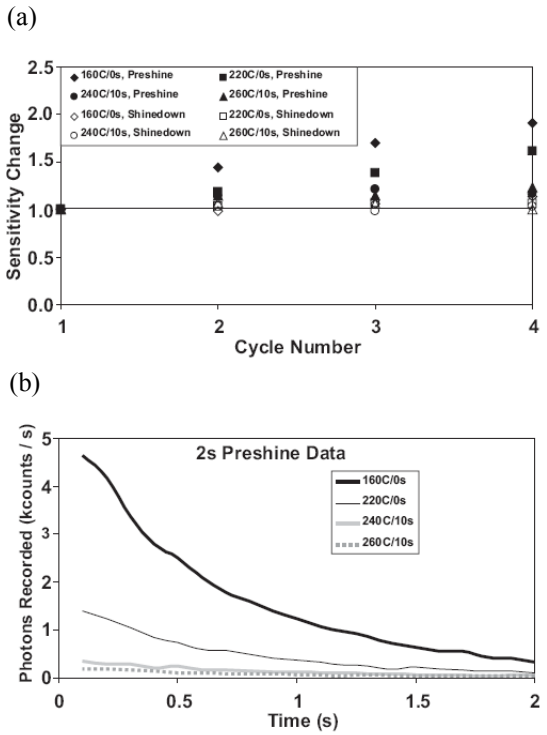

Figure 7: *a) Sensitivity change as a function of cutheat and preheat temperature and cycle number. b) Preshine data (0.35 mW.cm^{-2} power) for the fourth cutheat and preheat cycle shown in Table 2.*

measurements, because generally a less stringent cutheat is used as opposed to preheat (Murray and Wintle, 2000). Jain et al. (2003) show that different OSL components do not always sensitize in the same manner.

Application to OSL samples, glacial Lake Hitchcock

Table 4 compares results for sample GLH-06-09-782 for the conventional SAR procedure with results for the modified SAR with preshine procedure (Table 3); data are included for all aliquots (0 rejected, criteria = none), and for aliquots rejected if recycling or D_e errors exceed 10% (criteria = 10%, data in boldface type). The average percent absolute error on the recycling ratio and average percent error on the equivalent dose are tabulated in Table 4; other rejection criteria were also monitored (test dose error, decay curve characteristics, feldspar contamination, D_e > regenerative doses), but have not been tabulated.

The conventional SAR procedure (Method: SAR) resulted in a large error on both tabulated criteria, and a large proportion of rejected aliquots (17 of 19 rejected). The preshine-SAR procedure (Method: ps-SAR) reduced the errors on these rejection criteria, and resulted in a smaller proportion of rejected aliquots (6 of 25 rejected). Finally, the conventional

Method	Rejected Aliquots (Criteria)[a]	Average Recycling Ratio, (%)[b]	Average D_e Error (%)[c]	D_e (± 1σ)[d]
SAR	0 of 19 (none)	0.87 (19%)	15.22	34.44 ± 3.60
SAR	**17 of 19 (10%)**	**0.98 (3%)**	**6.10**	**21.86 ± 2.92**
ps-SAR	0 of 25 (none)	0.96 (8%)	5.04	32.76 ± 2.83
ps-SAR	**6 of 25 (10%)**	**0.97 (5%)**	**4.35**	**29.83 ± 1.10**
ps-SAR (150-180µm)	**14 of 40 (10%)**	**1.01 (5%)**	**4.76**	**29.77 ± 1.22**
SAR, omit channel 1	0 of19 (none)	1.05 (13%)	22.93	23.13 ± 1.97
SAR, omit channel 1	**15 of 19 (10%)**	**1.05 (6%)**	**3.18**	**29.53 ± 4.38**

Notes:
a: Rejection criteria (none = no aliquots rejected, 10% = aliquots with recycling ratio and De error >10%); other rejection criteria were also monitored
b: Average percent absolute error on the recycling ratio
c: Average percent error on the equivalent dose
d: 1 standard error
90-125 or 90-150µm grains, unless otherwise noted

Table 4: *OSL data for the Cushman Delta (GLH-06-09-782) sample. Data selected/rejected using normal (i.e. 10%) rejection criteria are in boldface type. Methods used are discussed in the text.*

Sample #	Lab #	Method	Aliquots[a]	Dose Rate	D_e (± 1σ)[b]	Age (ka)
DELTAIC DEPOSITS, 14-18 ka[c]:						
Cushman Delta (strong ultrafast)						
GLH-06-09-782	UNL-558	SAR	2 of 19	2.02 ± 0.05	21.86 ± 2.92	10.8 ± 1.5
GLH-06-09-782	UNL-558	ps-SAR	19 of 25	2.02 ± 0.05	29.83 ± 1.10	14.8 ± 0.8
GLH-06-09-782	UNL-558	ps-SAR (150-180µm)	26 of 40	2.02 ± 0.05	29.77 ± 1.22	14.7 ± 0.8
DUNE DEPOSITS, < 14 ka[c]						
Hadley dune on lake bottom (weak ultrafast)						
GLH-06-09-779	UNL-556	SAR	11	1.47 ± 0.05	17.80 ± 1.49	12.1 ± 1.1
GLH-06-09-779	UNL-556	ps-SAR	21	1.47 ± 0.05	16.97 ± 0.81	11.6 ± 0.7
GLH-06-09-781	UNL-557	ps-SAR	19	1.81 ± 0.06	19.51 ± 1.09	10.8 ± 0.8
Montague echo dune on early terrace cut into Montague delta (weak ultrafast)						
GLH-07-03-89-3	UNL-554	ps-SAR	21	1.37 ± 0.04	18.16 ± 0.73	13.3 ± 0.8
South Hadley dune on Chicopee delta						
GLH-06-03-778	UNL-555	ps-SAR	28	2.08 ± 0.06	25.74 ± 1.46	12.4 ± 0.9

Notes:
a: Aliquot rejection based on D_e error, recycling ratio, test dose error, decay curve characteristics, feldspar contamination, D_e > regenerative doses
b: 1 standard error
c: Age constraints from varve and radiocarbon chronology
ps-SAR: SAR following a 3s 1 % power CW-OSL preshine
grain size is 90-125 or 90-150µm, unless otherwise noted

Table 5: *Comparison of optical ages of samples from Glacial Lake Hitchcock determined using SAR and ps-SAR with a 1% diode power (0.35 mW cm^{-2}) 3 s preshine.*

SAR data were recalculated but channel 1 (0.17s; total power 31.5 mW.cm^{-2}), which should contain the ultrafast component, was omitted (Method: SAR, omit channel 1). This produced a data set with large errors on the D_e values and a large number of rejected aliquots (15 of 19 rejected). The large number of rejected aliquots is believed to be due to removal of not only the ultrafast component, but also a large proportion of the fast component from this low response sample. The D_e values determined using normal rejection criteria and the preshine-SAR (both 90-150 and 150-180μm), and conventional SAR omitting channel 1 are almost identical, and differ significantly from the conventional SAR (channel 1 included) of the data (Table 4). However, the preshine-SAR is the only technique which did not result in a large number of rejected aliquots.

Samples from Glacial Lake Hitchcock were re-analyzed using the modified SAR with preshine sequence (Table 3). Results are shown in Table 5. SAR dose rates were determined as outlined in Rittenour et al. (2003, 2005) using the cosmic dose rate equations of Prescott and Hutton (1994) and the dose rate conversion factors of Adamiec and Aitken (1998). Errors were calculated in quadrature using the methods of Aitken and Alldred (1972) and Aitken (1976, 1985). Only sample GLH-06-09-782 showed the presence of a strong ultrafast component, although a weak ultrafast component was detected in three other samples. Using the SAR technique with a 0.35 mW.cm^{-2} (1%) 3s preshine increased the determined age for sample GLH-06-09-782 by 4 ka, beyond the combined 1-sigma error bars.

The ultrafast component in GLH-06-09-782 showed grain-size dependency, and was not detected in LM-OSL studies of the coarser 150-180 and 180-212μm fractions, although subsequent preshine-SAR analyses showed it to be present as a minor component. The coarser fraction was analyzed using the preshine-SAR method, with results which are consistent with preshine-SAR data from the 90-150μm fraction (ps-SAR, Table 5). The SAR with preshine ages for all samples are consistent with varve and radiocarbon age constraints from the lake basin (see below).

Comparison of OSL ages to other age constraints

Samples for OSL dating were collected from a high-stand delta of Glacial Lake Hitchcock and several post-drainage sand dunes from the lake bottom, an early terrace and an abandoned delta surface. These samples were carefully selected to bracket the timing of lake drainage within central Massachusetts.

In addition to the fairly well-dated NE varve chronology (Ridge et al., 1999, 2001), the timing of ice retreat, duration of lake existence, and the timing of lake drainage in central Massachusetts are constrained by a varve-sequence core collected from the University of Massachusetts-Amherst campus (UMass core, Figure 1b) (Rittenour, 1999; Rittenour et al., 1999; Rittenour and Brigham-Grette, 2000). The UMass core extends to 32m depth below the lake bottom surface and covers a sequence of 1,389 varves that transition from thick pro-glacial varves immediately above bedrock to thin distal varves at the top of the sequence. A radiocarbon age obtained from a sample collected near the top of the core (NE varves 5761-5768, 12,370 ± 120 ^{14}C yr BP, Beta 124780; ~14.5 ± 0.5 cal ka using INTCAL04, Reimer et al., 2004) indicates that the UMass core covers the interval from 15.6 – 14.2 ± 0.5 cal ka, consistent with the chronology of Ridge et al. (1999). Based on this core and the NE varve chronology, the ice margin retreated north of Amherst MA by 15.6 ± 0.5 cal ka (first varve deposited over bedrock) and Glacial Lake Hitchcock drained in this region sometime after 14.2 ± 0.5 cal ka (last varve deposited in core) (Rittenour, 1999), providing a narrower time frame for the duration of lake existence in central Massachusetts than the entire length of the varve chronology (4000 years).

Assuming the UMass core chronology and the NE varve chronology are correct, deltas into Glacial Lake Hitchcock could only have formed after ice retreat from the region but before lake drainage (15.6-14.2 ± 0.5 cal ka), and sand dunes on the lake bottom, early terraces and abandoned deltas could only have formed after the lake drained (after 14.2 ± 0.5 cal ka). The OSL ages obtained from the preshine-SAR method are consistent with these age constraints and indicate that topset beds from the Cushman Delta (GLH-06-09-782) are 14.7-14.8 ± 0.8 ka and sand dunes in the region formed between 13.3 ± 0.8 cal ka and 10.8 ± 0.8 ka (Table 5).

Conclusions

The following conclusions can be made with respect to the LM-OSL study of samples from Glacial Lake Hitchcock:

1. Blue LM-OSL background is a rising curve modelled with a third-order polynomial. Voltage applied to the stimulating LEDs is linear, within the error of the measurements.

2. A strong ultrafast component present in sample GLH-06-09-782 from Glacial Lake Hitchcock was preferentially removed using a 0.35 mW. cm^{-2} (1%) power 3s CW-OSL sequence prior to

each OSL measurement in the SAR protocol. This produced a reduction in the ultrafast component similar to a stringent 300°C/20s preheat, but with much less relative reduction in the fast component.

3. Differential sensitivity changes in the preshine data are observed as a function of stringency of cutheat and preheat. This results in inappropriate sensitivity corrections in the conventional SAR procedure, since prior heating is different for regenerative and test doses. This is reflected in problems with the recycling ratio and equivalent dose errors, and results in a large number of rejected D_e determinations based upon these criteria. If a preshine is not used to remove the ultrafast, the cutheat and preheat conditions must be the same, as noted by Packman et al. (in press). However, that will still lead to erroneous D_e values because of the presence of the thermally unstable ultrafast component in regenerative OSL data but its absence in the natural OSL data (Jain et al. 2003).

4. The improvement in errors in calculated D_e and recycling ratio criteria using a preshine are due to the correction of the differential sensitivity change between test-dose and regenerative-dose data, whereas changes in the D_e values will also be due in part to removal of the unstable ultrafast from the regenerative dose as opposed to natural data. The use of a preshine drastically reduced the rejection rate for D_e determinations.

5. OSL curves measured subsequent to the preshine show no sensitivity dependency upon cutheat/preheat conditions (160°C/0s, 220°C/0s, 240°C/10s, 260°C/10s).

6. Optical ages determined using the SAR procedure with a preshine are compatible with varve and radiocarbon age constraints.

Acknowledgements

We thank Mayank Jain for helpful comments on the early stages of this research and for rigorous and helpful review of the manuscript, and Julie Brigham-Grette for assistance in the field and supervision of the M.S. research from which this project developed. This research was supported in part by a University of Nebraska-Lincoln Maud Hammond Fling Faculty Research Fellowship to R.J. Goble.

References

Adamiec, G. and Aitken, M. (1998) Dose-rate conversion factors: update. *Ancient TL* **16**, 37-50.

Aitken, M.J. (1976) Thermoluminescent age evaluation and assessment of error limits: revised system. *Archaeometry* **18**, 233-238.

Aitken, M.J. (1985) *Thermoluminescence Dating*. Academic Press, London.

Aitken, M.J. and Alldred, J.C. (1972) The assessment of error limits in thermoluminescent dating. *Archaeometry* **14**, 257-267.

Antevs, E. (1922) The recession of the last ice sheet in *New England: American Geographical Society Research Series* **11**.

Bøtter-Jensen, L., Bulur, E., Duller, G.A.T. and Murray, A.S. (2000) Advances in luminescence instrument systems. *Radiation Measurements* **32**, 523-528.

Bulur, E., Bøtter-Jensen L. and Murray, A.S. (2000) Optically stimulated luminescence from quartz measured using the linear modulation technique. *Radiation Measurements* **32**, 407-411.

Choi, J.H., Duller, G.A.T. and Wintle, A.G. (2006) Analysis of quartz LM-OSL curves. *Ancient TL* **24**, 9-20.

Choi, J.H., Murray, A.S., Jain, M., Cheong, C.-S. and Chang, H.W. (2003) Luminescence dating of well-sorted marine terrace sediments on the southeastern coast of Korea. *Quaternary Science Reviews* **22**, 407-421.

Jain, M., Murray, A.S. and Bøtter-Jensen, L. (2003) Characterisation of blue-light stimulated luminescence components in different quartz samples: implications for dose measurement. *Radiation Measurements* **37**, 441-449.

Murray, A.S. and Wintle, A.G. (2000) Luminescence dating of quartz using an improved single-aliquot regenerative-dose protocol. *Radiation Measurements* **32**, 57-73.

Murray, A.S. and Wintle, A.G. (2003) The single aliquot regenerative dose protocol: potential for improvements in reliability. *Radiation Measurements* **37**, 377-381.

Packman, S.C., Mauz, B., Rousseau, D.-D., Antoine, P., Rossignol, J. and Lang, A. (in press) Implications of broad dose distributions obtained with the single-aliquot regenerative-dose method on quartz fine-grains from loess. *Quaternary Geochronology*

Prescott, J.R. and Hutton, J.T. (1994) Cosmic ray contributions to dose rates for luminescence and ESR dating: large depths and long-term time variations. *Radiation Measurements* **23**, 497-500.

Reimer P.J., Baillie, M.G.L., Bard, E., Bayliss, A., Beck, J.W., Bertrand, C., Blackwell, P.G., Buck,

C.E., Burr, G., Cutler, K.B., Damon, P.E., Edwards, R.L., Fairbanks, R.G., Friedrich, M., Guilderson, T.P., Hughen, K.A., Kromer, B., McCormac, F.G., Manning, S., Bronk Ramsey, C., Reimer, R.W., Remmele, S., Southon, J.R., Stuiver, M., Talamo, S., Taylor, F.W., van der Plicht, J. and Weyhenmeyer C.E. (2004) IntCal04 terrestrial radiocarbon age calibration, 0-26 cal kyr BP. *Radiocarbon* **46**, 1029-1058.

Ridge, J.C. (2003) The last deglaciation of the northeastern United States: A combined varve, paleomagnetic, and calibrated ^{14}C chronology: In: D.L. Cremeens and J.P. Hart Eds., *Geoarchaeology of Landscapes in the Glaciated Northeast*, New York State Museum Bulletin **397**, 15-45.

Ridge, J.C., Besonen, M.R. Brochu, M. Brown, S.L. Callahan, J.W. Cook, G.J. Nicholson, R.S. and Toll, T.J. (1999) Varve, paleomagnetic, and ^{14}C chronologies for Late Pleistocene events in New Hampshire and Vermont, U.S.A.. *Geographie physique et Quaternaire* **53**, 1-31.

Ridge, J.C., Canwell, B.A., Kelley, M.A. and Kelley, S.Z. (2001) Atmospheric ^{14}C chronology for late Wisconsin deglaciation and sea-level change in eastern New England using varve and paleomagnetic records: In: T.K Weddle and M.J. Retelle Eds., Deglacial History and Relative Sea-level Changes, Northern New England and Adjacent Canada, Special Paper No. 351, Geological Society of America, Boulder, CO, p. 173-191.

Rittenour, T.M. (1999) *Drainage History of Glacial Lake Hitchcock, Northeastern United States*, Unpublished Masters Thesis, Department of Geosciences, University of Massachusetts, Amherst, 179 p.

Rittenour, T.M. and Brigham-Grette, J. (2000) A Drainage History for Glacial Lake Hitchcock: Varves, Landforms, and Stratigraphy: In: J. Brigham-Grette Ed. North Eastern Friends of the Pleistocene Field Guidebook, Dept of Geosciences Contribution No. 7, University of Massachusetts, Amherst, 125 p.

Rittenour, T.M. Brigham-Grette, J. and Mann, M.E. (2000) El Nino-like climate teleconnections in New England during the Late Pleistocene. *Science* **288**, 1039-1042.

Rittenour, T.M. Goble, R.J. and Blum, M.D. (2003) An optical age chronology of late Pleistocene fluvial deposits in the northern lower Mississippi valley. *Quaternary Science Reviews* **22**, 1105-1110.

Rittenour, T.M. Goble, R.J. and Blum, M.D. (2005) Development of an OSL chronology for Late Pleistocene channel belts in the lower Mississippi valley, USA. *Quaternary Science Reviews* **24**, 2539-2554.

Singarayer, J.S. and Bailey, R.M. (2003) Further investigations of the quartz optically stimulated luminescence components using linear modulation. *Radiation Measurements* **37**, 451-458.

Reviewer

Mayank Jain